An Extension of the Student's T-distribution Mixture Model and the Gradient Descent Method

Taisong Xiong and Jianping Gou
School of Computer Science and Engineering, University of Electronic Science and Technology of China, Chengdu, 611731, P. R. China
Email: {xiongtaisong, cherish.gjp}@gmail.com
Yunbo Rao
School of Information and Software Engineering, University of Electronic Science and Technology of China. Chengdu, Sichuan, 610054, P.R China.
Email: cloudrao@gmail.com

***Abstract*—A new Student's t-distribution finite mixture model is proposed which incorporates the local spatial information of the pixels. The pixels' label probability proportions are explicitly modelled as probability vectors in the proposed model. We use the gradient descend method to estimate the parameters of the proposed model. Comprehensive experiments are performed for synthetic and natural grayscale images. The experimental results demonstrate that the superiority of the proposed model over some other models.**

***Index Terms*—Spatially variant finite mixture model, Student's t-distribution, Image segmentation, Gradient descent**

I. Introduction

Image segmentation is one of the most widely studied problems in computer vision. Its goal is to find the group of pixels. In statistics, image segmentation is referred to as cluster analysis [1]. Image segmentation has beep successfully applied to many applications. For example, it is used to identify the diatoms [2], simulated pattern painting [3], vehicle type recognition [4] and medical image segmentation [5].

The finite mixture model (FMM) [6], [7], a widely applied clustering model, provides a flexible method to model many random phenomena. The FMM can be applied to image segmentation because the k clusters can be generated by the k components of the FMM. The component function of the FMM can be various statistical distributions. The FMM is called Gaussian mixture model (GMM) if its component function is Gaussian distribution. The FMM has received increasing attention in the past decade. It has been widely applied to many fields, such as biology, economics, psychiatry, engineering and image segmentation [6]. When it is used for image segmentation, it assumes that the pixels are independent of each other. However, the probability of the pixels belonging to the same class is larger if the positions of the pixels are nearer.

In order to resolve the aforementioned shortcoming of the FMM, G.S.Sanjay [8] proposed a novel spatially variant finite mixture model (SVFMM) which incorporated the spatial relationships between the pixels. The SVFMM is different from the Markov random field (MRF) models in [9], [10], the former model imposes the MRF on the label probability vectors (the probabilities of each pixel belonging to some classes), the latter model imposes the MRF on the label probability vector priors. Compared to the MRF models, the SVFMM can reduce the complexity and computational cost of the model. The parameters of SVFMM are usually estimated by Expectation-Maximization (EM) [11] algorithm. Subsequently, some models based on SVFMM have been proposed and applied to medical imaging segmentation [12], [13]. Markov Chain Monte Carlo (MCMC) and Variational Bayes (VB) [7], [14] approximation inference algorithm are used to estimate the parameters of these models .

However, it cannot obtain closed form solutions of the label probability vectors in the M-step of the EM. A reparatory computation is adopted to project the solutions onto the unit simplex (positive and summing up to one components). A gradient projection algorithm is utilized in [8]. Convex quadratic programming is proposed for the SVFMM in [15] and better segmentation results are obtained in [15] than in [8]. But the MRF prior of the SVFMM in [8] and in [15] is not adaptive the data. A Gauss-Markov random field prior is proposed in [16] and imposed on the label probability vectors. The parameters of the model can be estimated from the data. However, the closed form solutions are still not obtained in this model.

Integrating the SVFMM with line processes [9], two variations of the SVFMM are proposed in [17]. In the two models, MRF smoothness priors are imposed on the label probability proportions of the two spatially varying Gaussian mixture models. The local differences between the label probability proportions of the two models are supposed to follow Gaussian distribution and continuous univariate Student's t-distribution, respectively. At the same time, Bernoulli distribution is imposed on the binary line processes (BLP) of the former model and Gamma distribution is imposed on the continuous line processes (CLP) of the latter model. A quadratic approximation is used to make the label probability vectors to be probability vectors. To avoid the projection step, a novel model based on GMM is proposed in [18] which incorporates the spatial information of the pixels. The label probability proportions are explicitly modeled as probability vectors.

doi:10.4304/jcp.8.7.1750-1757

The pixel value is replaced with the mean value of its neighboring pixels value in the representation of its label probability proportion. Gradient descent method is used to estimate the model parameters. We refer to the model in [18] as spatial neighborhood GMM (SNGMM).

In the aforementioned models, the component functions all are Gaussian distribution. However, the Gaussian distribution cannot meet the needs for many applications because its tails are too short. The student's t-distribution owns heavier tailed and is more robust [19], [20] against noise than Gaussian distribution. In the past few years, the student's t-distribution has been successfully applied to signal analysis [21], speaker identification [22] and image segmentation [23].

To consider the robustness of the student's t-distribution and the advantages of SVFMM, we propose a SVFMM whose component function is student's t-distribution in this paper. At the same time, the label probability proportions of the proposed model are explicitly modeled as probability vectors. Gradient descent method is used to estimate the model parameters instead of the EM algorithm. The experiments are conducted on both synthetic and natural grayscale images. To quantify the effectiveness of image segmentation, the misclassification ratio (MCR) [24] and the probabilistic rand (PR) index [25] are adopted. The experimental results demonstrate that the effectiveness and robustness of the proposed method compared with the other state-of-the-art models.

The remainder of this paper is organized as follows. We introduce the SVFMM and Student's t-distribution in brief in Section II. In Section III, the proposed model is described in detail. In Section IV, we give the experimental results conducted on both synthetic and natural grayscale images to evaluate the efficiency of the proposed model. Finally, the conclusions are given in Section V.

II. The Related Works

In this section, we first review SVFMM in brief, then the Student's t-distribution is introduced briefly. In this paper, we use x_n to denote the pixel in the *n*th position of an image.

A. Spatially variant finite mixture model

The SVFMM which incorporates the spatial information of pixels is an extension of FMM [8], [23]. It uses label probability proportion π_{nk} to denote the probability that the *n*th pixel belongs to the *k*th class. The variable π_{nk} must satisfy the following constraints

$$0 \le \pi_{nk} \le 1, \sum_{k=1}^{K} \pi_{nk} = 1; n = 1, ..., N, k = 1, ..., K.$$

Let π^n represent the *n*th pixel's label probability vector. The parameter vector π^n is equal to $(\pi_{n1}, \pi_{n2}, ..., \pi_{nK})^T$, where T indicates the transpose of a vector. Let $\Pi=\{(\pi^1)^T, (\pi^2)^T, ..., (\pi^N)^T\}$ be the set of probability vectors, and $\Theta = \{\theta_1, \theta_2, ..., \theta_K\}$ be the set of component parameters. The density function of the *n*th pixel is defined as follows

$$f(x_n|\Pi, \Theta) = \sum_{k=1}^{K} \pi_{nk} p(x_n|\theta_k).$$

In general, the component function is Gaussian distribution where parameter $\theta_k = \{\mu_k, \sigma_k^2\}$ and μ_k and σ_k^2 represent the mean and the variance of Gaussian distribution, respectively. The observations X consist of a data set $\{x_n\}$, where n=1, ..., N. The X's probability density function (PDF) [8] is given by

$$f(X|\Pi, \Theta) = \prod_{n=1}^{N} f(x_n|\Pi, \Theta). \quad (1)$$

A Gibbs distribution function is imposed on the parameter set Π in [15], which is given by

$$p(\Pi) = \frac{1}{Z}\exp(-U(\Pi)), \text{ with } U(\Pi) = \beta \sum_{n=1}^{N} V_{N_n}(\Pi),$$

where Z is a normalizing constant and β is a regularization parameter. The function $V_{N_n}(\Pi)$ denotes the clique potential function within the neighborhood N_n. According to Bayes' theorem, a posteriori PDF is derived as follows when the prior density is given.

$$p(\Pi|X; \Theta) \propto \prod_{n=1}^{N} p(\Pi) f(x_n|\Pi, \Theta).$$

Then the log-density function is given by [15]

$$\log(\Pi|X; \Theta) = \sum_{n=1}^{N} \log \sum_{k=1}^{K} \pi_{nk} p\left(x_n|\mu_k, \sigma_k^2\right) + \log p(\Pi) \quad (2)$$

In general, the EM algorithm is used to estimate the unknown parameters in (2). However, the results of the π_{nk} obtained in the M-step of the EM algorithm usually do not satisfy these constraints: $0 \le \pi_{nk} \le 1$ and $\sum_{k=1}^{K} \pi_{nk} = 1$. To enforce the label probability proportion π_{nk} to satisfy these constraints, in the M-step of EM algorithm a reparatory computation is in general added. When the unknown parameters are determined, the label obtained by the maximum a posteriori (MAP) estimation according to the posterior probability $p(\theta_k|x_n)$ in (3) is assigned to the pixel x_n.

$$p(\theta_k|x_n) = \frac{\pi_{nk} p(x_n|\theta_k)}{\sum_{j=1}^{K} \pi_{nj} p(x_n|\theta_j)}. \quad (3)$$

B. The Student's t-distribution

We assume that a random variable x follows a univariate Student's t-distribution $x \sim St(x|\mu, \lambda, \nu)$. Its definition is written in the following form [7]

$$St(x|\mu, \lambda, \nu) = \frac{\Gamma(\nu/2 + 1/2)}{\Gamma(\nu/2)} \left(\frac{\lambda}{\pi\nu}\right)^{1/2} \times \left[1 + \frac{\lambda(x-\mu)^2}{\nu}\right]^{-\nu/2-1/2}, \quad (4)$$

where μ and λ are the mean and the precision of the Student's t-distribution, respectively. $\Gamma(\cdot)$ represents a gamma function. The parameter ν is called the degrees of freedom of the Student's t-distribution. As ν tends to infinity, the t-distribution tends to a Gaussian distribution with the same mean μ and precision λ [7]. Therefore, the tails of the Student's t-distribution are longer than the Gaussian distribution.

III. The Proposed Model

In this section, we propose an extension of the Student's t-distribution mixture model which incorporates the spatial information of the image pixels. In the proposed model, we adopt a second-order neighborhood system to represent the spatial relationships of the pixels.

First, we adopt a function defined in [26] to represent the weight of the *n*th pixel belonging to the *k*th class

$$\xi_k(x_n) = \sum_{x_i \in N_n} \exp\left(-\frac{(x_i - c_k)^2}{2b_k^2}\right) \tag{5}$$

where N_n represents the neighborhood of the *n*th pixel. A new pixel's label probability proportion π_{nk} which incorporates its spatial relationships between other pixels is given by [26]

$$\pi_{nk} = \frac{\xi_k(x_n)}{\sum_{j=1}^{K} \xi_j(x_n)} = \frac{\sum_{x_i \in N_n} \exp\left(-\frac{(x_i - c_k)^2}{2b_k^2}\right)}{\sum_{j=1}^{K} \sum_{x_i \in N_n} \exp\left(-\frac{(x_i - c_j)^2}{2b_j^2}\right)}. \tag{6}$$

Obviously, the value of the label probability proportion π_{nk} in (6) is nonnegative and subjects to $\sum_{k=1}^{K} \pi_{nk} = 1$. The density function of the *n*th pixel is given by

$$f(x_n|\theta) = \sum_{k=1}^{K} \pi_{nk} St(x_n|\theta_k), \tag{7}$$

where the component function $St(x_n|\theta_k)$ is the Student's t-distribution defined in (4), its parameters are $\theta_k = \{\mu_k, \lambda_k\}$. According to Bayes' theorem, the posterior probability is derived as follows

$$f(\theta_k|x_n) = \frac{\pi_{nk} St(x_n|\theta_k)}{\sum_{j=1}^{K} \pi_{nj} St(x_n|\theta_j)}. \tag{8}$$

The log-likelihood function is defined as follows

$$L(\theta) = \sum_{n=1}^{N} \log f(x_n) = \sum_{n=1}^{N} \log\left(\sum_{k=1}^{K} \pi_{nk} St(x_n|\theta_k)\right). \tag{9}$$

Then our objective is to estimate the parameters $\Omega = \{\mu_k, \lambda_k, c_k, b_k^2\}$ with respect to the maximization of the log-likelihood function. Since the logarithm function is a monotonically increasing function, the error function is adopted here which is defined the negative logarithm of the log-likelihood function [7].

$$J(\Omega) = -L(\Omega) = -\sum_{n=1}^{N} \log\left(\sum_{k=1}^{K} \pi_{nk} St(x_n|\theta_k)\right). \tag{10}$$

Applying the complete data, the change of the error function is given by

$$J(\Omega^{(t+1)}) - J(\Omega^{(t)}) = -\sum_{n=1}^{N} \log\left(\frac{\sum_{j=1}^{K} \pi_{nj} St(x_n|\theta_j)}{\sum_{k=1}^{K} \pi_{nk} St(x_n|\theta_k)} \times \frac{f^{(t)}(\theta_j|x_n)}{f^{(t)}(\theta_j|x_n)}\right). \tag{11}$$

Because the $St^{(t)}(\theta_j|x_n)$ always satisfies the conditions: $St^{(t)}(\theta_k|x_n) \geq 0$ and $\sum_{k=1}^{K} St^{(t)}(\theta_k|x_n) = 1$. According to the Jensen's inequality [27], the change of the error function in (11) is obtained as follows:

$$J(\Omega^{(t+1)}) - J(\Omega^{(t)}) \leq -\sum_{n=1}^{N} \sum_{k=1}^{K} St^{(t)}(\theta_k|x_n) \times \log\left(\frac{\pi_{nk}^{(t+1)} St^{(t+1)}(x_n|\theta_k)}{St^{(t)}(\theta_k|x_n) \sum_{j=1}^{K} \pi_{nj}^{(t)} St^{(t)}(x_n|\theta_j)}\right). \tag{12}$$

The terms which depend on the old parameters (at the *t*th iteration step) are dropped when we minimize the log-likelihood function with respect to the new parameters (at the *t+1*th iteration step). The change in error function is rewritten as follows

$$E\left(\Omega^{(t)}|\Omega^{(t+1)}\right) = -\sum_{n=1}^{N} \sum_{k=1}^{K} St^{(t)}(\theta_k|x_n) \times \log\left(\pi_{nk}^{(t+1)} St^{(t+1)}(x_n|\theta_k)\right). \tag{13}$$

The E in (13) can be referred to as an error function. Therefore, we minimize E in (13) instead of maximizing the log-likelihood function (9). To minimize the error function E, we utilize the derivatives of the function with respect to μ_j, λ_j, c_j, b_j^2, which can be calculated by

$$\frac{\partial E}{\partial \mu_j} = -\sum_{n=1}^{N} St^{(t)}(\theta_j|x_n) \cdot \frac{\lambda_j(\nu+1)(x_n - \mu_j)}{\nu + \lambda_j(x_n - \mu_j)^2}. \tag{14}$$

$$\frac{\partial E}{\partial \lambda_j} = -\sum_{n=1}^{N} St^{(t)}(\theta_j|x_n) \cdot \frac{\nu - \nu \times \lambda_j(x_n - \mu_j)^2}{2\lambda_j[\nu + \lambda_j(x_n - \mu_j)^2]}. \tag{15}$$

$$\frac{\partial E}{\partial c_j} = -\sum_{n=1}^{N} St^{(t)}(\theta_j|x_n) \cdot \frac{\sum_{x_i \in N_n} \frac{(x_i - c_j)}{b_j^2} \cdot \exp\left(-\frac{(x_i - c_j)^2}{2b_j^2}\right)}{\sum_{x_i \in N_n} \exp\left(-\frac{(x_i - c_j)^2}{2b_j^2}\right)} + \sum_{n=1}^{N} \sum_{k=1}^{K} St^{(t)}(\theta_k|x_n) \cdot \frac{\sum_{x_i \in N_n} \frac{(x_i - c_j)}{b_j^2} \cdot \exp\left(-\frac{(x_i - c_j)^2}{2b_j^2}\right)}{\sum_{p=1}^{K}\left[\sum_{x_i \in N_n} \exp\left(-\frac{(x_i - c_p)^2}{2b_p^2}\right)\right]}. \tag{16}$$

$$\frac{\partial E}{\partial b_j^{(2)}} = -\sum_{n=1}^{N} St^{(t)}\left(\theta_j|x_n\right) \cdot \frac{\sum\limits_{x_i \in N_n} \frac{(x_i-c_j)^2}{2b_j^4} \cdot \exp\left(-\frac{(x_i-c_j)^2}{2b_j^2}\right)}{\sum\limits_{x_i \in N_n} \exp\left(-\frac{(x_i-c_j)^2}{2b_j^2}\right)} + \sum_{n=1}^{N}\sum_{k=1}^{K} St^{(t)}\left(\theta_k|x_n\right) \cdot \frac{\sum\limits_{x_i \in N_n} \frac{(x_i-c_j)^2}{2b_j^4} \cdot \exp\left(-\frac{(x_i-c_j)^2}{2b_j^2}\right)}{\sum\limits_{p=1}^{K}\left[\sum\limits_{x_i \in N_n} \exp\left(-\frac{(x_i-c_p)^2}{2b_p^2}\right)\right]}. \tag{17}$$

After the optimization of the parameters of the error function, the value of the posterior probability (8) is determined. Then according to MAP, the *n*th pixel obtains its class label by solution of

$$\arg\max_k \left\{f\left(\theta_k|x_n\right)\right\}. \tag{18}$$

The proposed model is called the spatially varying Student's t-distribution mixture model (SVStMM). We use gradient descend method to estimate the unknown parameters instead of the EM algorithm used in many models. The proposed model SVStMM is summarized in Algorithm 1.

Algorithm 1 SVStMM .

Initialize:

Use K-means to get the mean u_j and the variance σ_j^2. Then set μ_j=u_j, λ_j=1/σ_j^2, c_j=u_j and b_j^2=σ_j^2.

Step 1:

Compute the Student's t-distribution $St(x_i|\theta_j)$ (4).

Calculate the weight function $\xi_j\left(x_i\right)$ (5).

Update the label probability proportion π_{ij} (6).

Compute the posterior probability $f\left(\theta_j|x_i\right)$, as given by (8).

Step 2:

Update the parameters $\Omega = (\mu_j, \lambda_j, c_j, b_j^2)^T$ by using the gradient descend method

$$\Omega^{(t+1)} = \Omega^{(t)} - \eta \nabla L(\Omega^{(t)}) \tag{19}$$

where η denotes the learning rate. We have set η= 10^{-5} for the proposed model. $\nabla E(\Omega)$ is the derivative of the function E with respect to Ω, where $\nabla E(\Omega)$=$\left[\partial E/\partial \mu_j, \partial E/\partial \lambda_j, \partial E/\partial c_j, \partial E/\partial b_j^2\right]^T$.

Step 3:

If the value of (9) changes significantly, set $\Omega^{(t)}$=$\Omega^{(t+1)}$, and return to step 1.

Step 4:

Evaluate the posterior probability $f\left(\theta_j|x_i\right)$ given in (18) to obtain the class labels of the pixels.

IV. Numerical Experiments

In this section, some experiments are conducted on synthetic and natural grayscale images to evaluate the effectiveness and robustness of the proposed model. The proposed model is compared with the K-means [7], GMM [6], SVFMM [15], DCASV [16], CLP, BLP [17] and SNGMM [18]. The models are all implemented in MATLAB. The source code of SVFMM can be available at http://www.cs.uoi.gr/kblekas/sw/MAPsegmentation.html. The source code of K-means, standard GMM, DCASV, CLP and BLP can be download from http://www .cs.uoi.gr/cnikou/. We implement the model SNGMM and the proposed model (SVStMM) in MATLAB(R2010a). We have selected $\nu = 0.001$ for the proposed model. According to (4), the value of λ must be nonnegative, so we use the absolute value of λ in (20). The loop of SVStMM is terminated when the percentage changed of (8) between two consecutive iterations is less than 10^{-5}, i.e, $|\Delta L/L| < 10^{-5}$.

To quantify image segmentation results, two criteria are adopted in these experiments. One criterion is the mis-classification ratio (MCR) [24] which is used to quantify the synthetic image segmentation results. Its definition is given by

$$\text{MCR} = \frac{\text{number of mis-classified pixels}}{\text{total number of pixels}}.$$

The values of MCR are bounded by the interval [0, 1], where lower values indicate better segmentation results. The other criterion is the probabilistic rand (PR) index [25] which is used to quantify the natural image segmentation results. The PR index measures consistency between two segmentation labels via an overlapping fraction. The definition of the PR is given by

$$\text{PR}\left(S_{test}, \{S_k\}\right) = \frac{2}{N(N-1)} \sum_{i<j} \left[c_{ij}p_{ij} + (1-c_{ij})(1-p_{ij})\right],$$

where c_{ij}=1 when the pixels *i* and *j* belong to the same cluster in the test image S_{test}, otherwise c_{ij}=0. The values of PR are bounded by the interval [0, 1], where the larger PR values indicate better segmentation results.

A. Synthetic Images

A three-class synthetic image shown in Fig.1(a) is used to demonstrate the robustness of the proposed model against noise. The image has 128×128 image resolution with luminance values [55, 115, 225]. The image shown in Fig.1(b) is obtained by corrupting the original image with the mixed noise. The image is first corrupted by Gaussian noise (0 mean, 0.01 variance), then the salt & pepper noise (sp=0.05) is added. The image segmentation results are shown in Fig.1(c)-(j), respectively. It can be seen from Fig.1 the proposed model reduces the noise significantly. The information of the edges and contours is kept very well in the segmentation results of the proposed model. To further test the effectiveness of the proposed model, the experimental results obtained with various levels of mixed noise are given in Table 1. In order to reduce the influence of the the randomness of the added noise and the sensitivity of the initialization, we conduct the every test 10 times and the averages of the results are given in Table I. It can be seen from Table I, the proposed model

has a lower MCR than any other model. The experiments indicate that the proposed model is more robust against noise than the other models.

In the second experiment, a synthetic four-class (K=4) image (128×128 image resolution) with luminance values [0, 85, 170, 255] is used to test which is shown in Fig.2(a). The image is first corrupted by Gaussian noise (0 mean, 0.005 variance), then the salt & pepper noise (sp=0.03) is added. The corrupted image is shown in Fig.2(b). The segmentation results of all models are shown in Fig.(c)-(j). It can be seen that the results of the mixture models which consider the spatial information are better than GMM. The proposed model obtains lower MCR than any other model. It demonstrates that the proposed model is more robust against noise compared with the other models. The averages of the segmentation results based on the image shown in Fig.2(a) which is corrupted by varying levels of noise are given in Table II. It can be seen from Table II, the proposed model yields a lower MCR and its effectiveness and robustness outperforms any other model under all levels of noise.

B. Natural Images

It is a difficult and challenging task to segment the natural images. It is also hard to provide a good model to segment objects such as humans, animals, trees, buildings, etc, for the image segmentation models. In this experiment, we choose some natural grayscale images taken from the Berkeley image segmentation database [28] to test for visual and quantitative purposes. Each image of the image database has 481×321 pixels. Several manual segmentation ground-truth images are provided for each image. In these test, some grayscale images with or without artificial noise are used to evaluate the performance of the proposed model (SVStMM), compared with K-means, GMM, SVFMM, DCASV, CLP, BLP and SNGMM.

Firstly, six images are chosen to apply to visual evaluation of the image segmentation results. The visual segmentation results of these images are shown in Fig.3. Three images without noise are shown in the first column to the third column of the first row in Fig.3, another three images corrupted by mixture noise are shown in the forth column to the sixth column of the first row in Fig.3. The last three images are first corrupted by Gaussian noise (0 mean, 0.002 variance) and then salt & pepper noise (sp=0.03) is added to corrupt the images. The segmentation results of the models are shown in the second row to the ninth row of the Fig.3. It can be seen from the image segmentation results of the images without noise, the information of the contours and edges of the segmentation results of the proposed model is kept very well compared with any other model. For example, there are three classes ($K = 3$) in the third image, they are "snow", "background" and "wolf". As can be seen, the proposed model can better classify with more detail along the sharp edge between the "background" and "snow", and the "snow" and the "wolf", as compared with the other models. As regards the segmentation results of the K-means, GMM, SVMM, DCASV, CLP, BLP and SNGMM of the images with mixture noise, the noise is not clearly reduced. Obviously, the proposed model reduces the noise significantly. There are two classes in the forth image, they are the sky and objects. There are much noise in the segmentation results except for the proposed model. The sky and the objects can be distinguished very well of the segmentation results of the proposed model. As concerns the sixth image, compared with these state-of-art models, the proposed model reduces the noise significantly and yields better segmentation result which characterizes by homogeneous segmentation regions and sharp segmentation boundaries.

Next, thirty images taken from the Berkeley image segmentation database without and with artificial noise are applied to quantitative evaluation. The PR value is used to quantify the segmentation results. The PR value of the segmentation results is given in Table III. It can be seen from Table III, the differences of the segmentation results of the images without noise are relatively small for all models. But under the noise conditions, the PR values of the proposed model are larger than any other model. The experiment indicates that the proposed model is more robust against noise than the other models. The label probability proportion model of the proposed model incorporates the effective spatial relationships between the pixels, therefore the proposed model produces better segmentation results.

V. CONCLUSIONS

In this paper, we propose an image segmentation model which takes into account the spatial information of the pixels. The component function is Student's t-distribution which is a robust alternative to Gaussian distribution. Furthermore, the pixels' label probability proportions are explicitly modelled as probability vectors, thus a reparatory project step is avoided. We use the gradient descend method to estimate the parameters of the proposed model. The experiments conducted on both the synthetic images with mixture noise and natural images with and without noise show that the proposed model obtains better results than some models. It proves that the effectiveness and correctness of the proposed model. It also demonstrates that the proposed model effectively captures the spatial relationships between the pixels in an image.

ACKNOWLEDGMENT

The authors would like to thank the anonymous reviewers for their valuable comments and suggestions, which greatly helped to improve both the technical content and the presentation quality of the paper. This work was supported by the National Natural Science Foundation of China under grant No. U1233108.

REFERENCES

[1] S.Richard, "Computer Vision: Algorithms and Applications", Springer, 2010.

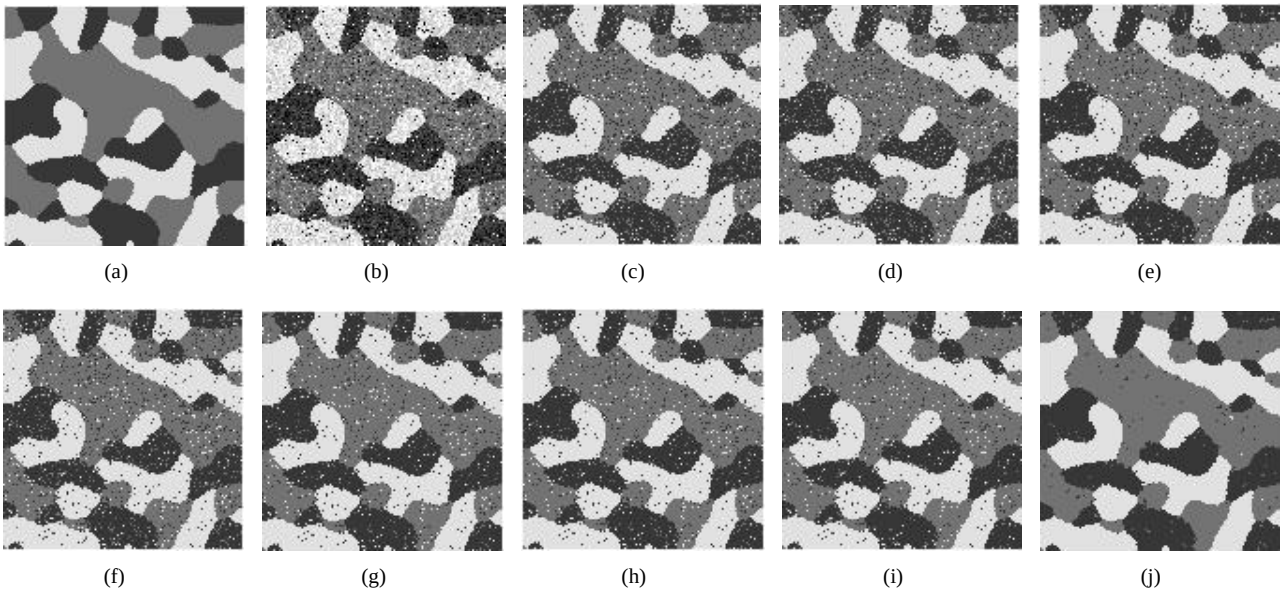

Fig. 1. First experiment (128×128 image resolution). (a)The original image. (b) Noise image with Gaussian noise (0 mean, 0.005 variance) and salt&pepper(sp=0.08). (c) K-means (MCR=11.73%). (d) GMM (MCR=11.73%). (e) SVFMM (MCR=8.26%). (f) DCASV (MCR=9.74%). (g) BLP (MCR=6.49%). (h) CLP (MCR=7.03%). (i)SNGMM (MCR=6.37%) (j) SVStMM (MCR=2.01%)

TABLE I
THE COMPARISON OF THE MCR FOR THE FIRST EXPERIMENT

Methods	Gaussian Noise(0 mean,var 0.01) + salt & pepper(sp)					
	sp=0.07	sp=0.09	sp=0.11	sp=0.13	sp=0.15	mean
K-means	13.05%	14.18%	15.57%	16.97%	18.46%	15.65%
GMM	13.08%	14.28%	15.75%	17.27%	18.85%	15.85%
SVFMM	9.55%	10.73%	12.19%	13.51%	15.09%	12.21%
DCASV	11.03%	12.23%	13.74%	15.25%	16.89%	13.83%
CLP	8.35%	9.72%	11.28%	12.74%	14.46%	11.31%
BLP	7.86%	9.24%	10.82%	12.31%	14.09%	10.86%
SNGMM	7.95%	9.63%	11.61%	13.53%	15.73%	11.69%
SVStMM	2.29%	2.67%	3.31%	4.09%	5.18%	3.51%

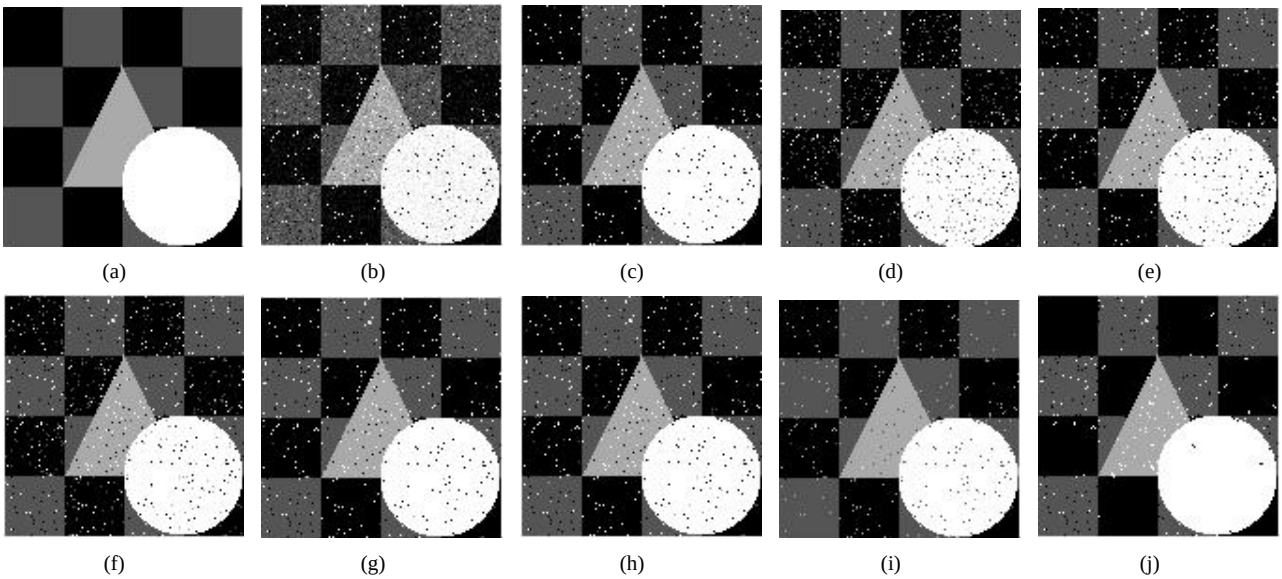

Fig. 2. Second experiment (128×128 image resolution). (a)The original image. (b) Noise image with Gaussian noise (0 mean, 0.005 variance) and salt&pepper(sp=0.03). (c) K-means(MCR=3.49%). (d) GMM (MCR=5.72%). (e) SVFMM (MCR=3.86%). (f) DCASV (MCR=4.21%). (g) BLP (MCR=2.89%). (h) CLP (MCR=2.69%). (i) SNGMM (MCR=2.08%) (j) SVStMM (MCR=1.65%)

[2] Q.Luo, Y.Gao, J.Luo, C.Chen, J.Liang and C.Yang "Automatic Identification of Diatoms with Circular Shape using Texture Analysis", *Journal of Software*, Vol.6, No.3, pp.428-435, 2012.

[3] J.Zhi, J.Liu, H.Yuan and G.Wu "Design of Simulated Pattern Painting Based on Image Segmentation and Recognition Method", *Journal of Software*, Vol.6, No.11, pp.2232-2238, 2011.

TABLE II
THE COMPARISON OF THE SECOND EXPERIMENT IN TERMS OF MCR

Methods	Gaussian Noise(0 mean,var) + salt & pepper(sp)					
	var=0.006 sp=0.05	var=0.007 sp=0.07	var=0.008 sp=0.09	var=0.009 sp=0.11	var=0.010 sp=0.13	mean
K-means	5.81%	8.20%	10.73%	13.41%	16.13%	10.86%
GMM	32.41%	33.27%	34.48%	35.62%	36.34%	34.22%
SVFMM	5.82%	8.27%	10.60%	12.77%	15.18%	10.53%
DCASV	6.98%	10.43%	13.77%	17.84%	22.26%	14.26%
CLP	4.68%	6.53%	8.67%	10.84%	13.30%	8.80%
BLP	4.37%	6.01%	7.98%	9.87%	12.21%	8.09%
SNGMM	3.46%	4.98%	6.92%	8.99%	11.24%	7.12%
SVStMM	2.61%	3.54%	4.78%	5.86%	7.67%	4.89%

Fig. 3. Segmentation examples of different methods based on the Berkeley segmentation grayscale database.The first row, from first column to the third column: the original images, from the fourth column to the sixth column, the original images corrupted by Gaussian noise (0 mean, 0.002 variance) and salt & pepper (sp=0.03). From the second row to the ninth row, each row shows: K-means, GMM, SVFMM, DCASV, CLP, BLP, SNGMM, SVStMM.

[4] W.Zhan and Z.Luo "Research of Vehicle Type Recognition System Based on Audio Video Interleaved Flow for Toll Station",*Journal*

TABLE III
COMPARISON OF SEGMENTATION RESULTS BASED ON BERKELEY GRAYSCALE IMAGES: PR INDEX.

Image	N	K	K-means	GMM	SVFMM	DCASV	CLP	BLP	SNGMM	SVStMM
167062	-	3	0.9505	0.8914	0.8999	0.9118	0.9162	0.9341	0.9284	0.9547
300091	-	2	0.6171	0.6186	0.6131	0.6180	0.6165	0.6164	0.6170	0.6189
126007	-	4	0.7187	0.7037	0.7231	0.7088	0.7172	0.7181	0.7130	0.7204
175032	-	6	0.5299	0.5305	0.5312	0.5307	0.5310	0.5313	0.5293	0.5316
260058	-	2	0.5802	0.5774	0.5830	0.5800	0.5801	0.5799	0.5840	0.5844
147091	-	2	0.7179	0.7031	0.7233	0.7141	0.7260	0.7255	0.7280	0.7324
145086	-	6	0.7688	0.7678	0.7688	0.7722	0.7720	0.7729	0.7745	0.7777
306005	-	6	0.7230	0.7052	0.7178	0.7128	0.7192	0.7228	0.7236	0.7233
241048	-	4	0.6857	0.6859	0.6872	0.6866	0.6866	0.6866	0.6870	0.6876
87046	-	5	0.6426	0.6487	0.6371	0.6454	0.6458	0.6455	0.6409	0.6460
55075	mn	4	0.7156	0.7284	0.7311	0.7308	0.7287	0.7291	0.7175	0.7451
41004	mn	4	0.6764	0.6912	0.6943	0.7025	0.7006	0.7046	0.6849	0.7214
198054	mn	3	0.6874	0.6799	0.6940	0.6844	0.7011	0.7033	0.6909	0.7365
66075	mn	2	0.6254	0.6133	0.6313	0.6083	0.6264	0.6250	0.6284	0.6609
94079	mn	3	0.5465	0.5573	0.5491	0.5601	0.5600	0.5627	0.5584	0.5842
138087	mn	3	0.6852	0.5064	0.6905	0.6813	0.6908	0.6914	0.6895	0.7218
67079	mn	2	0.6230	0.6286	0.6487	0.6374	0.6489	0.6507	0.6473	0.6939
227046	mn	4	0.7033	0.7006	0.7082	0.7064	0.7095	0.7098	0.7154	0.7308
97017	mn	2	0.7054	0.7037	0.7173	0.7090	0.7153	0.7155	0.7165	0.7825
311068	mn	2	0.7709	0.7843	0.7604	0.7928	0.7904	0.7958	0.7816	0.8703
147021	mn	3	0.6651	0.6438	0.7051	0.6918	0.7042	0.7062	0.7122	0.7490
23025	mn	3	0.6704	0.6807	0.6934	0.6886	0.6901	0.6912	0.6854	0.7152
189011	mn	2	0.6988	0.7043	0.7122	0.7068	0.7116	0.7121	0.7116	0.7716
126039	mn	3	0.6518	0.6503	0.6560	0.6528	0.6566	0.6570	0.6312	0.6841
113016	mn	2	0.6519	0.6896	0.6937	0.6995	0.7084	0.7136	0.6861	0.7439
238011	mn	3	0.7042	0.7120	0.7411	0.7305	0.7573	0.7649	0.7940	0.7996
106025	mn	3	0.6449	0.6361	0.6460	0.6357	0.6444	0.6434	0.6455	0.6758
43070	mn	2	0.7712	0.7718	0.7809	0.7751	0.7794	0.7785	0.7791	0.8275
112082	mn	4	0.6658	0.6634	0.6708	0.6729	0.6808	0.6825	0.6807	0.7003
105019	mn	2	0.7676	0.7914	0.8203	0.7778	0.8258	0.8257	0.8146	0.8918
mean	-	-	0.6855	0.6790	0.6943	0.6908	0.6980	0.6999	0.6966	0.7261

of Software, Vol.7, No.4, pp.741-744, 2012.

[5] T.Nguyen and Q.M.Wu, "Robust Student's-t Mixture Model With Spatial Constraints and Its Application in Medical Image Segmentation",*IEEE Transaction Mededical Imaging*, Vol.31, No.1 pp.103-116, 2012.

[6] G.McLachlan and D.Peel, "Finite Mixture Models", Wiley and Sons, New York, 2000.

[7] C.Bishop, "Pattern Recognition and Machine Learning", Springer, 2006.

[8] GS.Sanjay, TJ.Hebert, "Bayesian pixel classification using spatially variant finite mixtures and the generalized EM algorithm", *IEEE Transaction Image Processing*, Vol.7, No.7, pp.1014-1028, 1998.

[9] S.Geman, D.Geman, "Stochastic relaxation, Gibbs distributions,and the Bayesian restoration of images", *IEEE Transactions on Pattern Analysis and Machine Intelligence*, Vol.6, No.6, pp.721-741, 1984.

[10] G.Celeux, F.Forbes and N. Peyrard, "EM procedures using mean field-like approximations for Markov model-based image segmentation", *Pattern Recognition*, Vol.36, No.1, pp.131-144, 2003.

[11] A.P.Dempster, N.m.Laird and D.B.Rubin, "Maximum likelihood from incomplete data via EM algorithm", *Journal of the Royal Statistical Society,Series B*, Vol.39, No.1, pp.1-38, 1977.

[12] M.Woolrich, T.Behrens, C.Bechkmann and S.Smith, "Mixture models with adaptive spatial regularisation for segmentation with an application to FMRI data", *IEEE Transactions on Medical Imaging*, Vol.24, No.1, pp.1-11, 2005.

[13] M.Woolrich and T.Behrens, "Variational Bayes Inference of Spatial Mixture Models for Segmentation", *IEEE Transactions on Medical Imaging*, Vol.25, No.10, pp.1380-1391, 2006.

[14] M.T.Jordan, Z.Ghabramani, T.S.Jaakkola and L.K.Saul, "An introduction to variational methods for graphical models", *Machine Learning*, Vol.37, pp.183-233, 1999.

[15] K.Blekas, A.Likas, N.Galatsanos and I.Lagaris, "A spatially constrained mixture model for image segmentation", *IEEE Transaction on Neural Network*, Vol.16, No.2, pp.494-498, 2005.

[16] C.Nikou, N.Galatsanos and A.Likas, "A class-adaptive spatially variant mixture model for image segmentation", *IEEE Transaction Image Processing*, Vol.16, No.4, pp.1121-1130, 2007.

[17] G.Sfikas, C.Nikou, N.Galatsanos and C.Heinrich, "Spatially varying mixtures incorporating line processes for image segmentation", *Journal of Mathematical Imaging and Vision*, Vol.36, pp.91-110, 2010.

[18] M.N.Thanh, and Q.M.Wu, "Gaussian-Mixture-Model-based Spatial Neighborhood Relationships for Pixel Labeling Problem", *IEEE Transactions on Systems, Man, And Cybernetics-Part B: Cybernetics*, Vol.42, No.1, pp.193-202, 2012.

[19] D.Peel and G.J.McLachlan, "Robust mixture modelling using the t distribution", *Statistics and Computing*, Vol.10, pp.335-344, 2000.

[20] M.Svensen and C.Bishop, "Robust Bayesian mixture modelling", *Neurocomputing*, Vol.64, pp.235-252, 2005.

[21] S.P.Chatzis, D.I.Kosmopoulos and T.A.Varvarigou, "Signal Modeling and Classification Using a Robust Latent Space Model Based on t Distributions", *IEEE Transactions on Signal Processing*, Vol.56, No.3, pp.949-963, 2008.

[22] S.P.Chatzis and D.I.Kosmopoulosc, "A Variational Bayesian Methodology for Hidden Markov Models utilizing Student's-t Mixtures", *Pattern Recognition*, Vol.44, No.1, pp.295-306, 2011.

[23] T.Xiong, Z.Yi and L.Zhang. "Grayscale Image Segmentation by Spatially Variant Mixture Model with Student's t-distribution", *Multimedia Tools and Applications.*

[24] Y.Zhang, M.Brady and S.Smith, "Segmentation of brain MR images through a hidden Markov random field model and the expectation maximization algorithm", *IEEE Transactions on Medical Imaging*, Vol.20, No.1, pp.45-57, 2001.

[25] R.Unnikrishnan, C.Pantofaru and M.Hebert, "Toward objective evaluation of image segmentation algorithms", *IEEE Transactions on Pattern Analysis and Machine Intelligence* , Vol.29, No.6, pp.929-944, 2007.

[26] M.N.Thanh, Q.M.Wu and S.Ahuja, "An Extension of the Standard Mixture Model for Image Segmentation", *IEEE Transaction on Neural Network*, Vol.21, No.1, pp.1326-1338, 2010.

[27] W.Rudin, "Real and Complex Analysis", 3rded. New York:McGraw-Hill, 1987.

[28] D.Martin, C.Fowlkes, D.Tal and J.Malik, "A database of human segmented natural images and its application to evaluating segmentation algorithms and measuring ecological statistics", *IEEE Conference on Computer Vision*, 2001, pp.416-423.